

Diffusion and Overhauser NMR Studies on Dicationic Palladium Complexes of BINAP

Devendrababu Nama, Daniele Schott, Paul S. Pregosin,* L. F. Veiros, and M. J. Calhorda

Laboratory of Inorganic Chemistry, ETH, Zürich, CH-8093 Switzerland, Centro de Química Estrutural, Complexo I, Instituto Superior Técnico, Avenida Rovisco Pais 1, 1049-001 Lisbon, Portugal, and Departamento de Química e Bioquímica, Faculdade de Ciências, Universidade de Lisboa, 1749-016 Lisbon, Portugal

Received April 21, 2006

PGSE diffusion, ^1H , ^{19}F Overhauser, and related 2-D NMR studies on several salts of the dications $[\text{Pd}(\text{H}_2\text{O})_2(\text{BINAP})]^{2+}$, $[\text{Pd}(\mu\text{-OH})(\text{BINAP})]_2^{2+}$, and $[\text{Pd}_2(\mu\text{-OH})(\mu\text{-NH}(p\text{-RC}_6\text{H}_4))(\text{BINAP})_2]$, $\text{R} = \text{Cl}$, CH_3 , MeO , and, in one case, $[\text{Pd}(\mu\text{-O}_2\text{PF}_2)(\text{BINAP})]_2(\text{PF}_6)_2$, are reported. These solution NMR results, together with DFT calculations, reflect on how the anion interacts with the cation, as well as the extent, and the solvent dependence of the ion pairing. The solid-state structure of $[\text{Pd}_2(\mu\text{-OH})(\mu\text{-}\{\text{NH}(p\text{-Tol})\})\text{-}(\text{BINAP})_2](\text{CF}_3\text{SO}_3)_2$ has been determined.

Introduction

There is an increasing interest in the effects of the anion on the chemistry of cationic transition metal complexes.^{1–4} These effects include both change of the observed product, e.g., when the complex is used as a catalyst,¹ and marked changes in the rates of the various reactions.^{2,3} In terms of effects on homogeneously catalyzed reactions, it is slowly becoming clear that no one single “anion effect” is responsible; rather, there can be mechanistic changes,¹ faster or slower decomposition pathways,³ differences in the amount of—and the structures of—ion pairs,⁵ and certainly possible direct coordination, i.e., the anion functions as a ligand. Perhaps additional phenomena, e.g., aggregation, are equally important.

The recent inorganic literature has made increasing use of NMR diffusion data.^{5–15} Pulsed field spin-echo (PGSE) methods are often employed,^{5,6} although others favor DOSY

techniques.¹⁵ In some studies, the emphasis is on recognizing some form of aggregation; for example, it can be shown that a catalytically active Zr species is associated with the cocatalyst MAO⁷ or, alternatively, that there is a solvent dependence of the structure of a lithium salt, e.g., LiPPh_2 or BuLi .^{16,17}

Perhaps the most promising diffusion applications concern ready recognition of the amount of ion pairing. When diffusion constants for the cation and anion can be measured, separately, then their respective magnitudes are revealing. For cations and anions of very different size (and in the absence of, for example, hydrogen bonding), the observation of identical D values usually results from complete ion pairing.¹⁸ If the two values are different, the extent of the difference reflects the degree of ion pairing. Taken together with NOE studies, one can frequently determine the structural details for the ion pair. Since diffusion constants (D values) are solvent dependent, it is routine to report hydrodynamic radii, r_{H} , which can be obtained from the Stokes–

(1) Fagnou, K.; Lautens, M. *Angew. Chem., Int. Ed.* **2002**, *41*, 27–47. Lautens, M.; Fagnou, K.; Yang, D. Q. *J. Am. Chem. Soc.* **2003**, *125*, 14884–14892.

(2) Smidt, S. P.; Zimmermann, N.; Studer, M.; Pfaltz, A. *Chem.–Eur. J.* **2004**, *10*, 4685–4693.

(3) Faller, J. W.; Fontaine, P. P. *Organometallics* **2005**, *24*, 4132–4138.

(4) Krossing, I.; Raabe, I. *Angew. Chem., Int. Ed.* **2004**, *43*, 2066–2090.

(5) (a) Valentini, M.; Ruegger, H.; Pregosin, P. S. *Helv. Chim. Acta* **2001**, *84*, 2833–2853. (b) Drago, D.; Pregosin, P. S.; Pfaltz, A. *Chem. Commun.* **2002**, 286–287. (c) Kumar, P. G. A.; Pregosin, P. S.; Schmid, T. M.; Consiglio, G. *Magn. Reson. Chem.* **2004**, *42*, 795–800. (d) Kumar, P. G. A.; Pregosin, P. S.; Vallet, M.; Bernardinelli, G.; Jassar, R. F.; Viton, F.; Kundig, E. P. *Organometallics* **2004**, *23*, 5410–5418. (e) Schott, D.; Pregosin, P. S.; Jacques, N.; Chavarot, M.; Rose-Munch, F.; Rose, E. *Inorg. Chem.* **2005**, *44*, 5941–5948. (f) Fernandez, I.; Martinez-Viviente, E.; Pregosin, P. S. *Inorg. Chem.* **2005**, *44*, 5509–5513. (g) Nama, D.; Anil Kumar, P. G.; Pregosin, P. S. *Magn. Reson. Chem.* **2005**, *43*, 246.250. (h) Fernandez, I.; Pregosin, P. S. *Magn. Reson. Chem.* **2006**, *44*, 76–82.

(6) Burini, A.; Fackler, J. P.; Galassi, R.; Macchioni, A.; Omary, M. A.; Rawashdeh-Omary, M. A.; Pietroni, B. R.; Sabatini, S.; Zuccaccia, C. *J. Am. Chem. Soc.* **2002**, *124*, 4570–4571. Binotti, B.; Macchioni, A.; Zuccaccia, C.; Zuccaccia, C. *Comments Inorg. Chem.* **2002**, *23*, 417–450. Stahl, N. G.; Zuccaccia, C.; Jensen, T. R.; Marks, T. J. *J. Am. Chem. Soc.* **2003**, *125*, 5256–5257. Zuccaccia, C.; Stahl, N. G.; Macchioni, A.; Chen, M. C.; Roberts, J. A.; Marks, T. J. *J. Am. Chem. Soc.* **2004**, *126*, 1448–1464. Zuccaccia, D.; Macchioni, A. *Organometallics* **2005**, *24*, 3476–3486.

(7) Babushkin, D. E.; Brintzinger, H. *J. Am. Chem. Soc.* **2002**, *124*, 12869–12873.

(8) Hayamizu, K.; Aihara, Y. *Electrochim. Acta* **2004**, *49*, 3397–3402.

(9) Hayamizu, K.; Aihara, Y.; Arai, S.; Price, W. S. *Electrochim. Acta* **2000**, *45*, 1313–1319. Hayamizu, K.; Akiba, E.; Bando, T.; Aihara, Y.; Price, W. S. *Macromolecules* **2003**, *36*, 2785–2792. Hallwass, F.; Engelsberg, M.; Simas, A. M. *J. Phys. Chem. A* **2002**, *106*, 589–594.

(10) Hallwass, F.; Engelsberg, M.; Simas, A. M.; Barros, W. *Chem. Phys. Lett.* **2001**, *335*, 43–49.

(11) Jaing, Q.; Ruegger, H.; Venanzi, L. M. *Inorg. Chim. Acta* **1999**, *290*, 64–79.

(12) Stoop, R. M.; Bachmann, S.; Valentini, M.; Mezzetti, A. *Organometallics* **2000**, *19*, 4117–4126.

(13) Olenyuk, B.; Lovin, M. D.; Whiteford, J. A.; Stang, P. J. *J. Am. Chem. Soc.* **1999**, *121*, 10434–10435.

(14) Mo, H. P.; Pochapsky, T. C. *J. Phys. Chem. B* **1997**, *101*, 4485–4486. Pochapsky, S. S.; Mo, H. P.; Pochapsky, T. C. *J. Chem. Soc., Chem. Commun.* **1995**, 2513–2514.

(15) Cabrita, E. J.; Berger, S.; Brauer, P.; Karger, J. J. *Magn. Reson.* **2002**, *157*, 124–131. Cabrita, E. J.; Berger, S. *Magn. Reson. Chem.* **2002**, *40*, S122–S127. Hori, A.; Kumazawa, K.; Kusukawa, T.; Chand, D. K.; Fujita, M.; Sakamoto, S.; Yamaguchi, K. *Chem.–Eur. J.* **2001**, *7*, 4142–414. Harris, R. K.; Kinnear, K. A.; Morris, G. A. *Chem. Commun.* **2001**, 2422–2423.

(16) Fernández, I.; Martínez-Viviente, E.; Pregosin, P. S. *Inorg. Chem.* **2004**, *43*, 4555–4557.

(17) Keresztes, I.; Williard, P. G. *J. Am. Chem. Soc.* **2000**, *122*, 10228–10229.

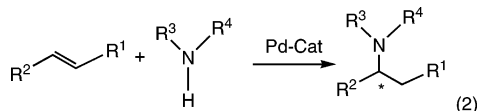
(18) Pregosin, P. S.; Kumar, P. G. A.; Fernandez, I. *Chem. Rev.* **2005**, *105*, 2977–2998. Pregosin, P. S.; Martinez-Viviente, E.; Kumar, P. G. A. *Dalton Trans.* **2003**, 4007–4014.

Einstein relation (eq 1),

$$r_H = \frac{kT}{6\pi\eta D} \quad (1)$$

where k is the Boltzmann constant, η is the viscosity of the solution, and T is the temperature.

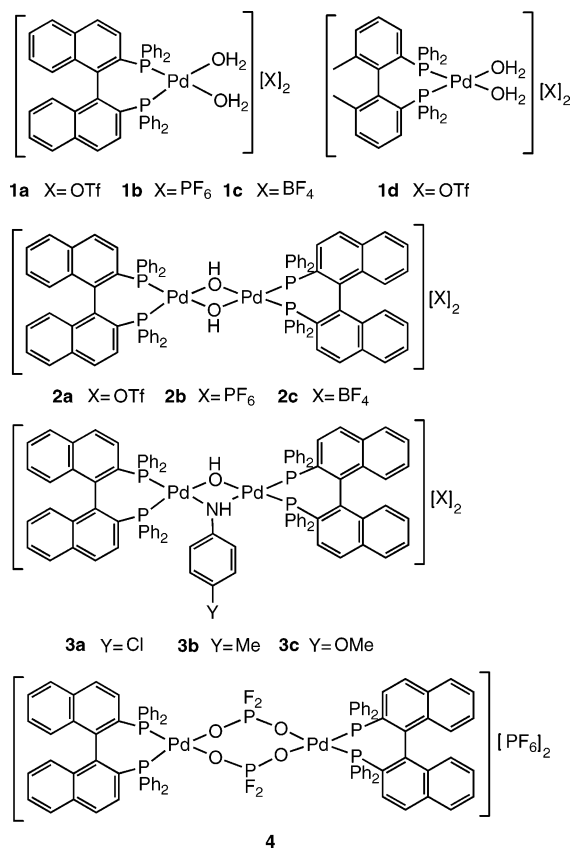
Cationic complexes of palladium are widely thought to be involved in a number of catalytic reactions including allylic alkylation,^{19,20} aldol condensations,²¹ ene-type Michael additions,²² and hydroamination^{23,24} (see eq 2), among others.



Sodeoka and co-workers,²³ and later Hii and co-workers,²⁴ have made extensive use of palladium BINAP and *p*-tolyl-BINAP dicationic aquo-complexes, $[\text{Pd}(\text{H}_2\text{O})_2(\text{BINAP})]^{2+}$ (**1**), as catalyst precursors in the enantioselective hydroamination reaction, indicated in eq 2. Occasionally, it has been found to be more convenient to use the hydroxo-bridged dicationic palladium salts, $[\text{Pd}(\mu\text{-OH})(\text{BINAP})]^{2+}$, **2**. Sometimes the BF_4 salts are used as precursors, and on other occasions, the triflate, CF_3SO_3^- , analogues. Important differences, in terms of yields and enantioselectivity, between these anions have been observed.²⁴

On the basis of our previous NMR and diffusion studies with aquo-complexes and triflate anions,²⁵ as well as our diffusion and ^1H , ^{19}F Overhauser measurements on the oxazoline palladium salt $[\text{Pd}((R,S)\text{-Bz-BIOX})(\text{CH}_3(\text{NCCH}_3))(\text{anion})]^{2+}$,²⁶ anion = BF_4^- , CF_3SO_3^- , and PF_6^- , and the allyl cations $[\text{Pd}(\eta^3\text{-CH}_3\text{-CHCHCHPh})(\text{dppe})]^{2+}$,²⁷ anion = BF_4^- , CF_3SO_3^- , BARF^- , and PF_6^- , we thought it likely that the salts of **1** and **2** might have different structures for the various anions. Moreover, given the reports by Sharp,²⁸ who has isolated a dinuclear bridging palladium hydroxo-anilide species, $[\text{Pd}_2(\mu\text{-OH})(\mu\text{-NHR})(\text{monodentate phosphine})_2]$, we were curious as to (a) the products of

Scheme 1. Pd-BINAP Salts^a



^a The analogous *p*-tolyl-BINAP salts are indicated in the text by a "prime", e.g., **2a'**.

the reaction of, for example, the dinuclear hydroxo-complex, **2**, with a suitable aniline and (b) how the anions would interact with differing bridging ligands.

We report here our diffusion and related NMR studies on the palladium BINAP (and *p*-tolyl-BINAP) complexes, **1–3**, presented in Scheme 1, and show that the PF_6 anion is readily hydrolyzed in the presence of the cation to afford the dicationic salt $[\text{Pd}(\mu\text{-O}_2\text{PF}_2)(\text{BINAP})]_2(\text{PF}_6)_2$, **4**.

Results and Discussion

The Pd-BINAP complexes were synthesized, as indicated in Scheme 2, by preparing the dichloride complex $\text{PdCl}_2(\text{BINAP})$ or *p*-tolyl-BINAP) and subsequently treating these neutral compounds with the appropriate silver salts to give the bis-aquo-derivatives. The dicationic aquo-complexes, **1**, can be converted to the bridging hydroxo-salts, **2**, by reaction with molecular sieves,²³ and the mono-anilide-bridged species, **3**, by addition of an aniline to the bridged hydroxo-complex.

NMR Characterization. The aquo-complexes, **1**, reveal a singlet in their ^{31}P spectra and broad proton resonances at ca. δ 3.0 (for the CF_3SO_3) and δ 4.1 (for the BF_4) for the two coordinated water molecules. The characterization of the dinuclear cations, **2**, was assisted by the recognition of the characteristic proton resonance for the $\mu\text{-OH}$ group at ca. -2.9 ppm.²³ Interestingly, all of the BINAP complexes reveal a rather broad aromatic proton resonance between 6 and 7 ppm. Earlier NMR studies^{29,30} have suggested that this signal is

(29) Trabesinger, G.; Albinati, A.; Feiken, N.; Kunz, R. W.; Pregosin, P. S.; Tschöner, M. *J. Am. Chem. Soc.* **1997**, *119*, 6315–6323. (30) Albinati, A.; Pregosin, P. S.; Salzmänn, R.; Albinati, A.; Kunz, R. W. *Organometallics* **1995**, *14*, 5160.

(19) Brown, J. M.; Hulmes, D. I.; Guiry, P. J. *Tetrahedron* **1994**, *50*, 4493–4506. (20) Trost, B. M.; Crawley, M. L. *Chem. Rev.* **2003**, *103*, 2921–2943. (21) Trost, B. M.; Shen, H. C.; Dong, L.; Surivet, J. P. *J. Am. Chem. Soc.* **2003**, *125*, 9276–9277. (22) Steinhagen, H.; Reggelin, M.; Helmchen, G. *Angew. Chem., Int. Ed. Engl.* **1997**, *36*, 2108–2110.

(23) Pregosin, P. S.; Salzmänn, R. *Coord. Chem. Rev.* **1996**, *155*, 35–68.

(24) Hatano, M.; Mikami, K. *J. Am. Chem. Soc.* **2003**, *125*, 4704–4706.

(25) Christoffers, J.; Baro, A. *Angew. Chem., Int. Ed.* **2003**, *42*, 1688–1690.

(26) (a) Fujii, A.; Sodeoka, M. *Tetrahedron Lett.* **1999**, *40*, 8011–8014. (b) Fujii, A.; Hagiwara, E.; Sodeoka, M. *J. Am. Chem. Soc.* **1999**, *121*, 5450–5458. (c) Hamashima, Y.; Hotta, D.; Sodeoka, M. *J. Am. Chem. Soc.* **2002**, *124*, 11240–11241. (d) Hamashima, Y.; Yagi, K.; Hisashi, T.; Tamas, I.; Sodeoka, M. *J. Am. Chem. Soc.* **2002**, *124*, 14530–14531. (e) Hamashima, Y.; Sodeoka, M. *Chem. Rec.* **2004**, *4*, 231–242. (f) Hamashima, Y.; Somei, H.; Shimura, Y.; Tamura, T.; Sodeoka, M. *Org. Lett.* **2004**, *6*, 1861–1864.

(27) (a) Li, K.; Hii, K. *Chem. Commun.* **2003**, 1132–1133. (b) Li, K.; Cheng, X.; Hii, K. *Eur. J. Org. Chem.* **2004**, 959–964. (c) Li, K. L.; Phua, P. H.; Hii, K. *Tetrahedron* **2005**, *61*, 6237–6242. (d) Phua, P. H.; de Vries, J. G.; Hii, K. *Adv. Synth. Catal.* **2005**, *347*, 1775–1780. (e) Phua, P. H.; de Vries, J. G.; Hii, K. *Adv. Synth. Catal.* **2006**, *348*, 587–592.

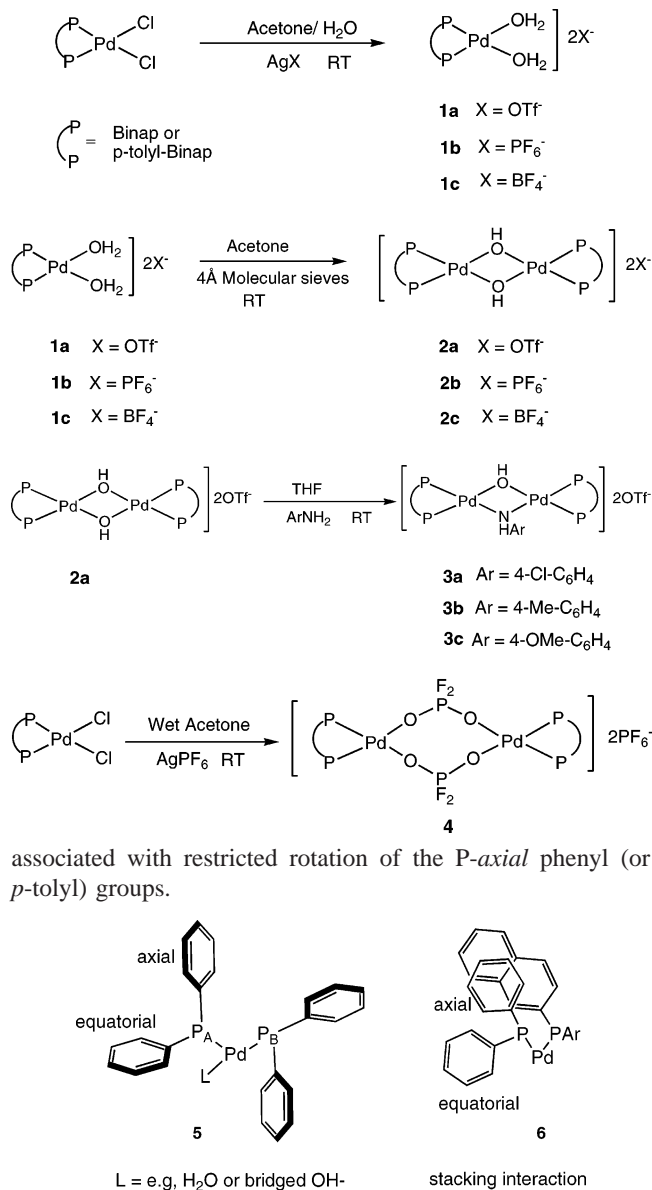
(28) Kumar, P. G. A.; Pregosin, P. S.; Goicoechea, J. M.; Whittlesey, M. K. *Organometallics* **2003**, *22*, 2956–2960.

(29) Sirbu, D.; Consiglio, G.; Milani, B.; Kumar, P. G. A.; Pregosin, P. S.; Gischig, S. *J. Organomet. Chem.* **2005**, *690*, 2254–2262.

(30) Schott, D.; Pregosin, P. S.; Veiros, L. F.; Calhorda, M. J. *Organometallics* **2005**, *24*, 5710–5717.

(31) (a) Anandhi, U.; Holbert, T.; Lueng, D.; Sharp, P. R. *Inorg. Chem.* **2003**, *42*, 1282–1295. (b) Kannan, S.; James, A. J.; Sharp, P. R. *Inorg. Chim. Acta* **2003**, *345*, 8–14.

Scheme 2. Syntheses of the Palladium Complexes



associated with restricted rotation of the P-axial phenyl (or *p*-tolyl) groups.

The axial P_A-aryl group (defined in fragment **5**) experiences a strong steric interaction with the naphthyl moiety associated with P_B (see **6**). In the solid state these aromatic moieties are usually "stacked".^{29–31} To confirm the source of the broad line, we have carried out low-temperature ¹H NMR measurements for the bridging hydroxide dinuclear *p*-tolyl salt, **2a'**, and show these in Figure 1. The choice of the *p*-tolyl analogues considerably simplifies the ¹H spectra and thus helps with the assignments for the conventional BINAP analogues. The broad signal at ca. 6.8 ppm disappears as the temperature is lowered and eventually splits into two nonequivalent *ortho*-protons, δ 8.00 and 6.72. At the same time two further new *meta* resonances appear, δ 7.21 and 6.25. At 213 K, the rotation about the P–C(ipso)_{axial} bond is slow and the new broad resonance at ca. 7.3 ppm corresponds to the equivalent *ortho*-protons of the equatorial P(*p*-tolyl) group. The integration and the various multiplicities are now in agreement with the proposed restricted rotation.

(30) Dotta, P.; Kumar, P. G. A.; Pregosin, P. S.; Albinati, A.; Rizzato, S. *Organometallics* **2004**, *23*, 2295–2304.

(31) Magistrato, A.; Pregosin, P. S.; Albinati, A.; Rothlisberger, U. *Organometallics* **2001**, *20*, 4178–4184.

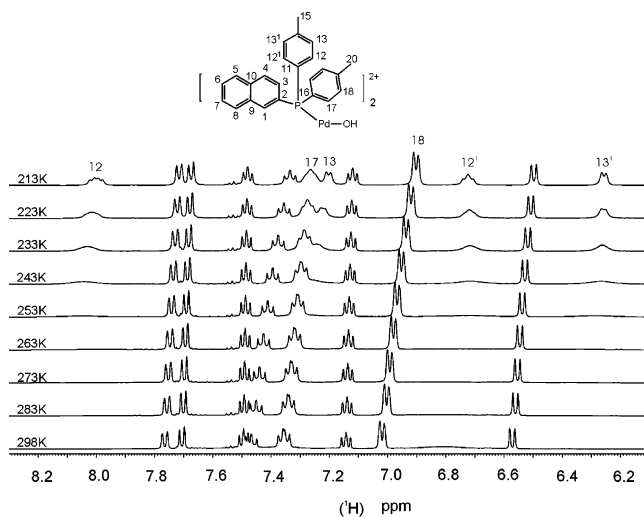


Figure 1. Variable-temperature NMR study for **2a'**. There is slow rotation around the P–C(ipso)_{axial} bond at ca. 213 K (CD₂Cl₂, 500 MHz).

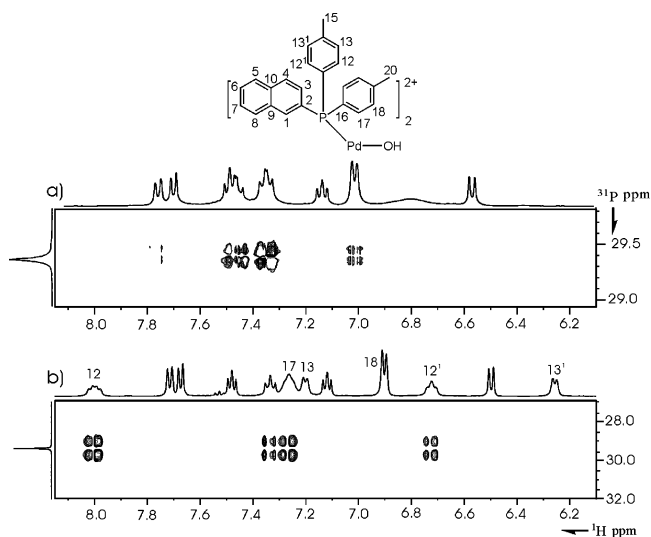


Figure 2. ³¹P,¹H correlation for **2a'** at ambient temperature (top) and (below) the same spectrum at 213 K (CD₂Cl₂, 500 MHz).

The ³¹P,¹H correlation for **2a'**, at 213 K, is given in the lower section of Figure 2 and reveals four sets of cross-peaks: two from the nonequivalent P-axial aryl *ortho*-protons, one from the equivalent P-equatorial aryl *ortho*-protons, and one set at 7.33 ppm for the naphthyl proton in *ortho* position to the P atom. The upper trace in Figure 2 shows the same correlation at ambient temperature. The broad resonance at ca. 6.8 ppm is visible; however only the strong cross-peaks from equivalent P-equatorial aryl *ortho*-protons and those from the *ortho* naphthyl proton are observed.³² Figure 3 shows a section of the ¹H,¹H NOESY for **2a'**. The proton from the bridged hydroxide, δ ca. –2.9, shows a strong cross-peak only with the equivalent P-equatorial aryl *ortho*-protons, plus a very strong *exchange* cross-peak with ca. 1 equiv of water, ca. δ 1.7. Table 1 shows the detailed ¹H assignments for this *p*-tolyl salt, **2a'**.

(32) There are weak contacts to the equatorial *meta*-protons. These same *meta*-protons also show a weak NOE interaction to the proton from the bridged hydroxide (see Figure 3).

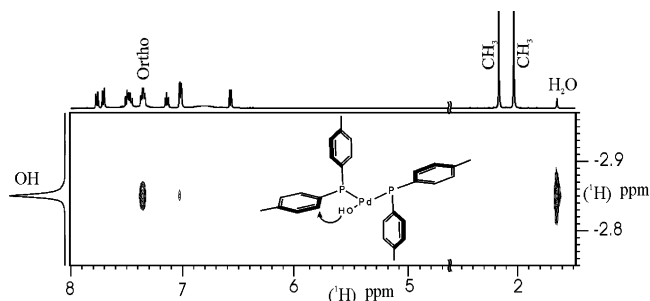
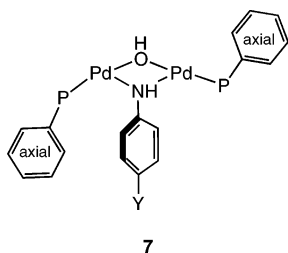


Figure 3. Section of the NOESY spectrum for **2a'** at ambient temperature revealing one strong contact to the *ortho*-protons of the equatorial P-phenyl ring and an exchange cross-peak with water (CD_2Cl_2 , 500 MHz).

Table 1. ^1H NMR Data for Complex **2a'** (CD_2Cl_2 , 500 MHz, 213 K)

position	δ ^1H
3	7.34
4	7.71
5	6.49
6	7.11
7	7.48
8	7.67
12	6.72
13	6.25
12 ¹	8.00
13 ¹	7.20
15	2.11
17	7.26
18	6.90
20	2.03
OH	-2.76

The NMR characterization for the bridging hydroxy-anilide dinuclear palladium complexes, **3**, was not trivial. Figure 4 (top) shows a typical ^{31}P NMR spectrum along with a simulation for this ABCD spin system. It is clear that the two ^{31}P -spins in *trans* positions to the $\mu\text{-OH}$ group are chemically different than the two ^{31}P -spins in *trans* positions to the $\mu\text{-NH}(p\text{-RC}_6\text{H}_4)$ moiety. The nonequivalence within, for example, the two ^{31}P -spins in *trans* positions to the $\mu\text{-OH}$ group arises due to the position of the bridging anilide ring with respect to the two axial (or equatorial) rings of the two PPh_2 groups. The solid-state structure for **3a**, shown in Figure 5, confirms that the anilide ring is proximate to one of these two axial rings, but remote from the second ring, thereby making all four ^{31}P -spins chemically nonequivalent (see 7).



The bridging OH protons appear at slightly lower frequency, ca. δ -3.7 to -4.0. Since the NH proton of the anilide does

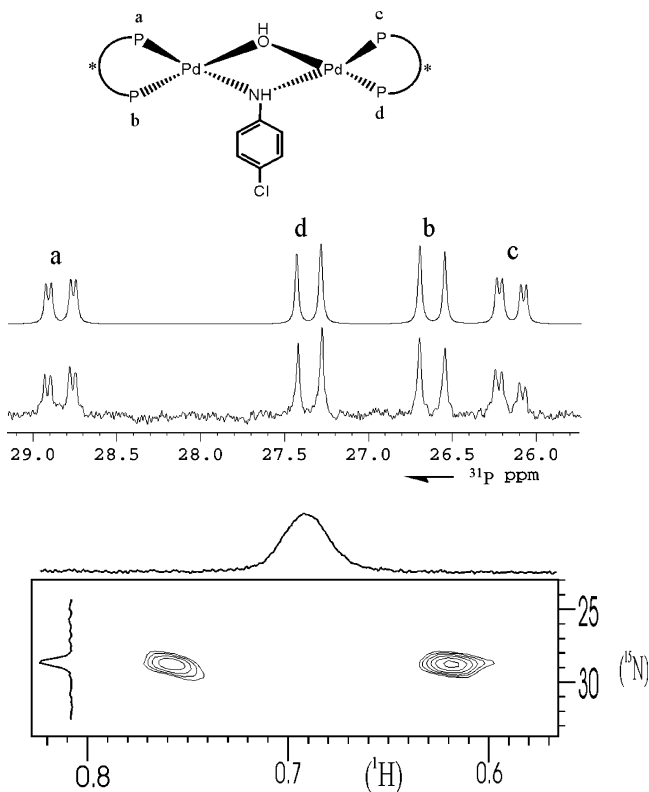


Figure 4. (top) Simulated and experimental ^{31}P spectra for salt **3a** in CD_2Cl_2 . $J_{ab} = 24.07$ Hz, $J_{ac} = 5.14$ Hz, $J_{cd} = 23.23$ Hz, $J_{bd} = 0.5$ Hz, $J_{bc} = 0.5$ Hz, $J_{ad} = 0.5$ Hz (400 MHz, 298 K). (bottom) ^{15}N , ^1H HMQC spectra for **3c** in CD_2Cl_2 (500 MHz, 213 K, δ $^{15}\text{N} = 52.5$ for the ligand $p\text{-MeO-C}_6\text{H}_4\text{NH}_2$).

not exchange very rapidly, this signal could be used to detect the nitrogen-15 chemical shift, in **3c**, via an HMQC spectrum (see Figure 4, bottom trace). We believe this (and the analogous measurement for **3a**) to be the first ^{15}N measurements on such bridging species. The ^{15}N chemical shift difference between the uncomplexed aniline and the coordinated $[\text{ArNH}]^-$ is 25.1 ppm.

Returning to the solid-state structure of the dication, $[\text{Pd}_2(\mu\text{-OH})(\mu\text{-}\{\text{NH}(p\text{-Tol})\})(\text{BINAP})_2](\text{CF}_3\text{SO}_3)_2$, **3b**, the local coordination geometry about each Pd atom is distorted square planar. The four-membered ring made up by the two Pd atoms and the bridging N and O atoms is not planar (see the caption to the figure); however, the four Pd-P bond lengths, Pd1-P1 223.5(2) pm, Pd1-P2 226.2(1) pm, Pd2-P3, 222.9(1) pm, and Pd2-P4 226.9(1) pm, are not very different and are relatively standard.³³ Further, the Pd1-O1, 204.9(4) pm, and Pd1-N1, 211.9(4) pm, bond lengths are as expected.³³ The two P-Pd-P angles, P1-Pd1-P2 92.32(5) $^\circ$ and P3-Pd2-P4 90.56(5) $^\circ$, are typical of Pd-BINAP complexes.^{34,35}

Dinuclear complex **4** is recognized via the observed multiplicities for the PF_2 moiety in the ^{31}P and ^{19}F spectra. This type of species has been reported on several occasions,^{28b,36,37} and it

(33) Orpen, A. G.; Brammer, L.; Allen, F. H.; Kennard, O.; Watson, D. G.; Taylor, R. J. *Chem. Soc., Dalton Trans.* **1989**, S1-S83.

(34) Mashima, K.; Kusano, K.; Ohta, T.; Noyori, R.; Takaya, H. *Binap J. Chem. Soc., Chem. Commun.* **1989**, 1208. Zhang, X.; Kazushi, M.; Koyano, K.; Sayo, N.; Kumobayashi, H.; Akutagawa, S.; Takaya, H. *Tetrahedron Lett.* **1991**, 32, 7283-7286. Zhang, X.; Mashima, K.; Koyano, K.; Sayo, N.; Kumobayashi, H.; Akutagawa, S.; Takaya, H. *J. Chem. Soc., Perkin Trans.* **1994**, 2309-2322. Ohkuma, T.; Koizumi, M.; Muniz, K.; Hilt, G.; Kabuto, C.; Noyori, R. *J. Am. Chem. Soc.* **2002**, 124, 6508-6509.

(35) Wiles, J. A.; Lee, C. E.; McDonald, R.; Bergens, S. H. *Organometallics* **1996**, 15, 3782-3784. Wiles, J. A.; Bergens, S. H. *Organometallics* **1999**, 18, 3709-3714.

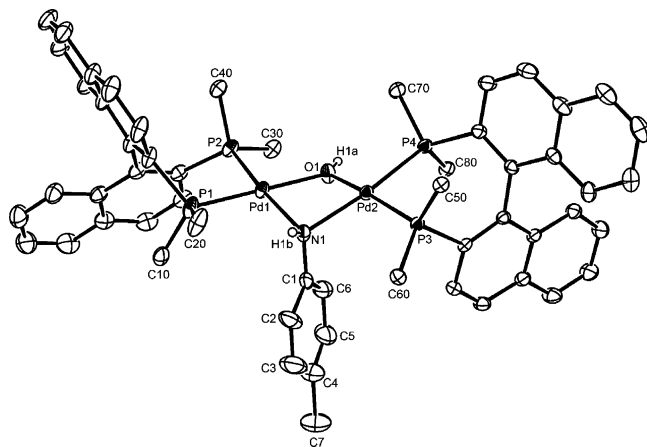


Figure 5. Structure of the dication $[\text{Pd}_2(\mu\text{-OH})(\mu\text{-}\{\text{NH}(p\text{-Tol})\})\text{-}(\text{BINAP})_2]$ in **3b**. Thermal ellipsoids are drawn at 30% probability; OTf^- anions and solvent molecules have been omitted for clarity. For the BINAP–P phenyl moieties only the *ipso*-carbon atom is shown. Bond lengths [pm] and angles [deg]: Pd1–P1 223.5(2), Pd1–P2 226.2(1), Pd1–O1 204.9(4), Pd1–N1 211.9(4), Pd1···Pd2 311.45(5), Pd2–P3 222.9(1), Pd2–P4 226.9(1), Pd2–O1 205.9(4), Pd2–N1 211.1(4), N1–C1 142.8(8), Pd1–N1–Pd2 94.8(2), N1–Pd1–O1 79.3(2), N1–Pd2–O1 79.3(2), Pd1–O1–Pd2 98.6(2), N1–Pd1–P1 96.9(1), N1–Pd1–P2 169.4(1), O1–Pd1–P2 91.8(1), O1–Pd1–P1 174.9(1), N1–Pd2–P3 102.2(1), N1–Pd2–P4 166.7(1), O1–Pd2–P4 87.5(1), O1–Pd2–P3 169.9(1), P1–Pd1–P2 92.32(5), P3–Pd2–P4 90.56(5); $\phi^1 = 6.5^\circ$, $\phi^2 = 10.3^\circ$; $\theta = 156.0^\circ$; $\phi^{1,2}$ is the intersection of the planes described by (1) P1, Pd1, P2 and O1, Pd1, N1 and (2) P3, Pd2, P4 and O1, Pd2, N1. θ is the intersection of the two L_4 -coordination spheres around Pd1 and Pd2.

is useful to note that it does not readily form in tetrahydrofuran (THF), but rather preferentially in dichloromethane (DCM) solution. Presumably, occasional weak palladium complexation (and/or H-bonding) of the PF_6^- ion will occur in dichloromethane solution, thereby facilitating the hydrolysis, whereas in THF, a solvent that is a much stronger ligand relative to dichloromethane, this process is suppressed.

Diffusion Studies. Tables 2–4 show PGSE diffusion data for the salts **1**–**4**. Not all of the salts were sufficiently soluble—or sufficiently stable—in the two solvents of interest, dichloromethane and THF.

For the BINAP cations of the di-aquo-salts, **1** (and the single Biphemp example³⁸), in dichloromethane solution, the corresponding r_H values fall in the range 6.2–6.9 Å (see Table 2). These radii are in good agreement with those estimated from Chem3D calculations (shown in Table 2, in parentheses). The corresponding radii for the CF_3SO_3^- anion, ca. 5.8–5.9 Å, are much too large for the isolated anion; nevertheless, the anion and cation are not moving at an identical rate. The BF_4^- anion also shows a similar r_H value.³⁹ The r_H values for both the CF_3SO_3^- and BF_4^- anions most likely result from a mixture of ion pairing and H-bonding of the anions to the complexed water molecules.

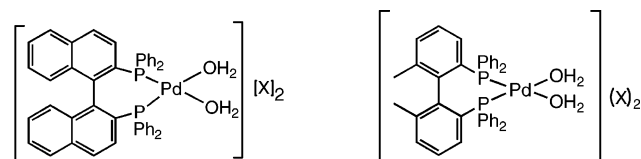
(36) Drago, D.; Pregosin, P. S. *Organometallics* **2002**, *21*, 1208–1215.

(37) (a) White, C.; Thompson, S. J.; Maitlis P. M. *J. Organomet. Chem.* **1977**, *134*, 319. (b) Connelly, N. G.; Einig, T.; Herbosa, G. G.; Hopkins, P. M.; Mealli, C.; Orpen, A. G.; Rosair, G. M.; Figuri, F. *J. Chem. Soc., Dalton Trans.* **1994**, 2025.

(38) We thank Prof. G. Consiglio, ETHZ, for the gift of the PdCl_2 (Biphemp).

(39) In dichloromethane solution one usually observes partial ion pairing; see ref 16.

Table 2. Diffusion Constants, D , and Hydrodynamic Radii, r_H , for the Pd Aquo-Complexes



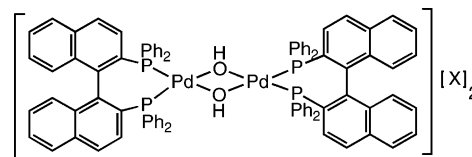
1a, X = OTf; **1b**, X = PF_6^- ; **1c** X = BF_4^-

1d X = OTf

compound		CD_2Cl_2		THF	
		D	r_H	D	r_H
1a , OTf	cation(^1H) BINAP	8.22	6.5 (6.4)	6.79	7.1
	anion(^{19}F)	9.26	5.8	7.70	6.3
1a' , OTf	cation(^1H) <i>p</i> -Tol-BINAP	7.79	6.9 (7.0)		
	anion(^{19}F)	9.32	5.8		
1b , PF_6^-	cation(^1H) BINAP			6.99	6.9
	anion(^{19}F)			10.25	4.7
1c , BF_4^-	cation(^1H) BINAP	8.33	6.4	6.83	7.1
	anion	8.78	6.1	7.04	6.8
1d , OTf	cation(^1H) Biphemp	8.62	6.2		
	anion(^{19}F)	9.03	5.9		

^a 400 MHz, 2 mM; D values, $10^{-10} \text{ m}^2 \text{ s}^{-1}$; r_H values, Å. Numbers in parentheses are calculated from Chem3D. $\eta(\text{CH}_2\text{Cl}_2) = 0.410 \times 10^{-3} \text{ kg m}^{-1} \text{ s}^{-1}$ at 300 K, $\eta(\text{THF}) = 0.456 \times 10^{-3} \text{ kg m}^{-1} \text{ s}^{-1}$ at 300 K.

Table 3. Diffusion Constants, D , and Hydrodynamic Radii, r_H , for the Bridged Hydroxy-Palladium Complexes, **2**



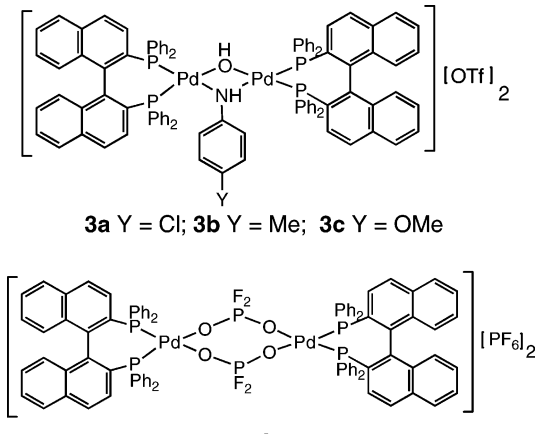
2a X = OTf **2b** X = PF_6^- **2c** X = BF_4^-

compound		CD_2Cl_2		THF	
		D	r_H	D	r_H
2a , OTf	cation(^1H) BINAP	6.63	8.1(8.1)	5.33	9.0
	anion(^{19}F)	9.40	5.7	5.94	8.1
2a' , OTf	cation(^1H) <i>p</i> -tol-BINAP	6.34	8.5(8.4)		
	anion(^{19}F)	9.43	5.7		
2b , PF_6^-	cation(^1H)	6.67	8.0		
	anion(^{19}F)	9.93	5.4		
2c , BF_4^-	cation(^1H) BINAP	6.67	8.0		
	anion(^{19}F)	9.76	5.5		
2c' , BF_4^-	cation(^1H) <i>p</i> -tol-BINAP	6.39	8.4		
	anion(^{19}F)	9.86	5.4		

^a 400 MHz, 2 mM; D values, $10^{-10} \text{ m}^2 \text{ s}^{-1}$; r_H values, Å. Numbers in parentheses are calculated from Chem3D. $\eta(\text{CH}_2\text{Cl}_2) = 0.410 \times 10^{-3} \text{ kg m}^{-1} \text{ s}^{-1}$ at 300 K, $\eta(\text{THF}) = 0.456 \times 10^{-3} \text{ kg m}^{-1} \text{ s}^{-1}$ at 300 K.

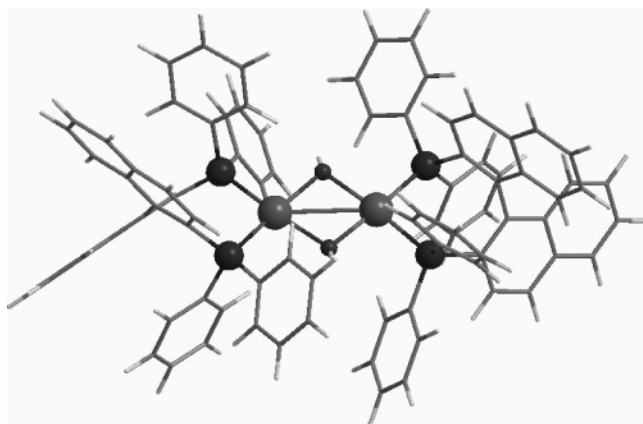
In THF solution the values for the cationic radii for **1a** and **1c** are larger and both 7.1 Å, whereas those for the anion are 6.3 and 6.8 Å, respectively. Ion pairing is usually more pronounced in THF than in dichloromethane;¹⁶ however, the larger solvent THF will also contribute to the increase in the cation r_H , relative to dichloromethane solutions. In any case, for **1a**, the percentage increase for cation and anion on going from dichloromethane to THF is ca. 9% ($7.1/6.5 = 1.092$; $6.3/5.8 = 1.086$). Taken together, these data for the three salts in THF solution provide a consistent picture for a mononuclear dication strongly, but not completely, associated with the anions.

DFT calculations⁴¹ were performed in order to assist in the interpretation of the HOESY results, which follow. The geometries of the two mononuclear complexes, the model cation

Table 4. Diffusion Constants, D , and Hydrodynamic Radii, r_H , for the Palladium-Bridged Anilide and PO_2F_2 Complexes


compound	CD_2Cl_2		THF		
	D	r_H	D	r_H	
3a	cation(^1H)	6.46	8.3	5.09	9.5
	anion(^{19}F)	9.49	5.6	5.89	8.2
3b	cation(^1H)	6.51	8.2 (8.3 ^b)	5.04	9.5
	anion(^{19}F)	9.56	5.6	6.41	7.6
3c	cation(^1H)	6.38	8.4	5.05	9.5
	anion(^{19}F)	9.32	5.7	5.81	8.3
4	cation(^1H)	6.06	8.8		
	anion(^{19}F)	9.81	5.5		

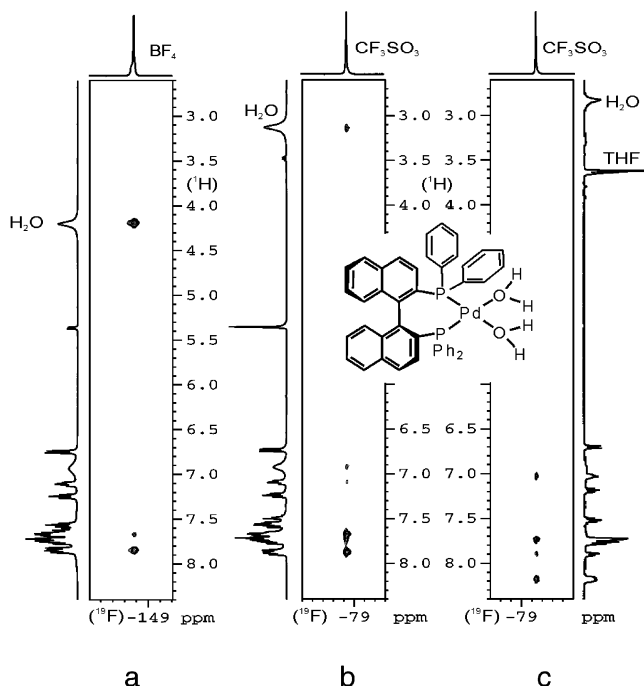
^a 400 MHz, 2 mM; D values, $10^{-10} \text{ m}^2 \text{ s}^{-1}$; r_H values, Å. $\eta(\text{CH}_2\text{Cl}_2) = 0.410 \times 10^{-3} \text{ kg m}^{-1} \text{ s}^{-1}$ at 300 K, $\eta(\text{THF}) = 0.456 \times 10^{-3} \text{ kg m}^{-1} \text{ s}^{-1}$ at 300 K. ^bFrom the X-ray data.

**Figure 6.** Optimized geometry (B3LYP) for $[\text{Pd}(\mu\text{-OH})(\text{BINAP})]_2^{2+}$. The Pd, P, and O atoms are highlighted.

$[\text{Pd}(\text{H}_2\text{O})_2(\text{Ph}_2\text{CH}_2\text{CH}_2\text{Ph}_2)]^{2+}$ and $[\text{Pd}(\text{H}_2\text{O})_2(\text{BINAP})]^{2+}$ (**1**), plus one dinuclear species, $[\text{Pd}(\mu\text{-OH})(\text{BINAP})]_2^{2+}$ (**2**), were fully optimized (see the Computational Details). The optimized structure of **2** is represented in Figure 6, whereas those corresponding to the mononuclear complexes are shown as Supporting Information (Figures S1 and S2), along with the atomic coordinates for all three complexes. In all cases, the coordination environment around each metal atom is square planar, as expected for Pd(II) complexes. The calculated Pd–P

(40) Stang, P. J.; Cao, D. H.; Poulter, G. T.; Arif, A. M. *Organometallics* **1995**, *14*, 1110–1114. The structure of the complex $[\text{Pd}(\text{H}_2\text{O})_2(\text{BINAP})]^{2+}(\text{CF}_3\text{SO}_3)_2$ has just been published (see ref 24e) and supports the proposed solution structure.

(41) Parr, R. G.; Yang, W. *Density Functional Theory of Atoms and Molecules*; Oxford University Press: New York, 1989.

**Figure 7.** HOESY spectra for (a) **1c** in CD_2Cl_2 , (b) **1a** in CD_2Cl_2 , and (c) **1a** in THF, all showing selective contacts to the equatorial P-phenyl ring protons. In (a) there is a strong contact to the bound water molecules.

distances (2.29 and 2.30 Å for dppe and 2.31–2.34 Å for BINAP) are close to the experimental values,⁴² as are those for Pd–O(H_2O) (2.22–2.25 Å) and Pd–O(OH) (2.09–2.10 Å) separations. Interestingly, the structure optimized for the dinuclear complex **2** confirms the proposed stacking interaction shown in **6**.

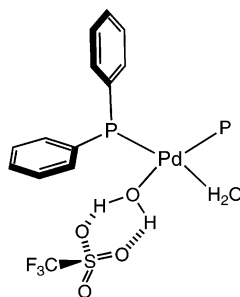
The charge distribution on the optimized complexes was evaluated by means of a natural population analysis (NPA),⁴³ and the atomic charges calculated for the metal and the coordinating atoms were for (a) the dppe complex, Pd: +0.36; P: +1.28/+1.30; O: –0.94/–0.95; (b) **1**, Pd: +0.37; P: +1.30; O: –0.95; and (c) **2**, Pd: +0.46/+0.47; P: +1.21 to +1.23; O: –1.00. In all three cases, the P atoms carry the largest amount of positive charge (1.0 to 1.2) and the palladium atoms possess considerably less positive charge (0.4 to 0.5). Although these results should not be taken as quantitative, they indicate that the anions are expected to seek out the P atoms, preferentially. The calculations performed do not account for the H-bonding associated with anions in the aquo-complexes,^{5c,25} but the NPA charges obtained allow a rationale for the results obtained from the dinuclear dications, **2–4**.

$^1\text{H}, ^{19}\text{F}$ HOESY spectra for the CF_3SO_3 salt, **1a**, in the two solvents are shown in sections b and c of Figure 7. The broad resonance for the two bound water molecules is clearly visible. In both solvents the strongest contacts from the fluorine of the anion arise from the equatorial P-phenyl aromatic protons. The

(42) See, for example, the Cambridge Structural Database (CSD): Allen, F. H. *Acta Crystallogr.* **2002**, *B58*, 380.

(43) (a) Carpenter, J. E.; Weinhold, F. *J. Mol. Struct. (THEOCHEM)* **1988**, *169*, 41. (b) Carpenter, J. E. Ph.D. Thesis, University of Wisconsin (Madison WI), 1987. (c) Foster, J. P.; Weinhold, F. *J. Am. Chem. Soc.* **1980**, *102*, 7211. (d) Reed, A. E.; Weinhold, F. *J. Chem. Phys.* **1983**, *78*, 4066. (e) Reed, A. E.; Weinhold, F. *J. Chem. Phys.* **1983**, *78*, 1736. (f) Reed, A. E.; Weinstock, R. B.; Weinhold, F. *J. Chem. Phys.* **1985**, *83*, 735. (g) Reed, A. E.; Curtiss, L. A.; Weinhold, F. *Chem. Rev.* **1988**, *88*, 899. (h) Weinhold, F.; Carpenter, J. E. *The Structure of Small Molecules and Ions*; Plenum: New York, 1988; p 227.

rather weak contact from the CF_3SO_3 fluorine to the water is somewhat surprising. Interestingly, in the solid-state structure for $[\text{Pd}(\text{H}_2\text{O})_2(\text{dppp})](\text{CF}_3\text{SO}_3)_2$,⁴⁰ in which the CF_3SO_3 is clearly hydrogen bonded to a complexed water ligand, the F–H distance is ca. 5.9 Å. Consequently, despite the absence of a strong Overhauser effect, we conclude that the anion is relatively strongly H-bonded (and therefore one finds relatively large r_{H} values) but situated quite close to one specific P-phenyl group, perhaps as indicated in **8**, thereby explaining the observed relaxation pathway.



8, fragment showing the proximity of the F-atoms to the equatorial P-phenyl.

The analogous HOESY spectrum for the BF_4 salt (Figure 7a) reveals a *strong* contact to the water molecules and a medium strength contact to the equatorial P-phenyl aromatic protons. Even though the residence time of the BF_4 anion is not 100%, based on the diffusion data, H-bonding via one of the F atoms (instead of the oxygen in the CF_3SO_3 anion) brings the anion close enough to the water protons so that this relaxation pathway dominates. In both salts, one finds a selective contact to the equatorial P-phenyl aromatic protons. We conclude that there is not a great deal of difference between the CF_3SO_3 and BF_4 anions in these salts, but this would not be obvious from the Overhauser spectroscopy alone.

For the bridging hydroxide salts, **2a–2c**, in dichloromethane solution, we find smaller D values and thus larger r_{H} values, relative to **1a–1c** (see Table 3). The ratio of D values (e.g., $8.22/6.63 = 1.24$) is in excellent agreement with ca. double the volume of **2a** relative to **1a**.^{5a} The r_{H} values of ca. 8.0–8.4 Å are in good agreement with estimations based on X-ray data. The few *p*-tolyl-BINAP salts, **2a'** and **2c'**, are, as expected, slightly larger due to the added methyl groups. The r_{H} values for the three anions, CF_3SO_3 , PF_6 , and BF_4 , are rather similar and, relative to the r_{H} values for the cations, modest in size. The r_{H} value for the CF_3SO_3 is now much smaller than in **1a**. The cation/anion ratio for **2a** is ca. 1.42, whereas this ratio for **1a** is 1.12. Assuming that the anions will prefer to avoid the (formally) negatively charged OH group, we assign these modest anion r_{H} values to 45–55% ion pairing, i.e., what one normally finds in dichloromethane solution for a number of different transition metal salts.¹⁶ For **2a** in THF solution the r_{H} values suggest a much larger percentage of ion pairing. There seems to be no important differentiation between these anions in these salts.

^1H , ^{19}F HOESY spectra for the *p*-tol BINAP CF_3SO_3 and BF_4 salts **2a'** and **2c'** are shown in Figure 8. The strongest contacts stem from the aromatic region, and these five to six cross-peaks can be assigned to protons from *both* the pseudoaxial and pseudoequatorial P-aryl groups. Indeed, there are also weak cross-peaks to both *p*-tolyl methyl groups. As expected, there is little or no contact to the low-frequency OH proton. Given

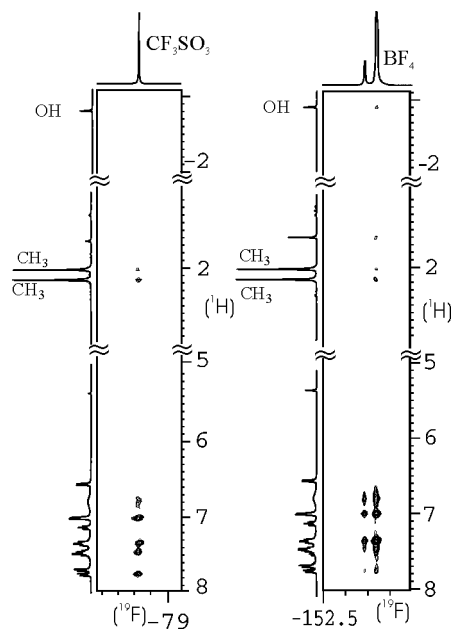
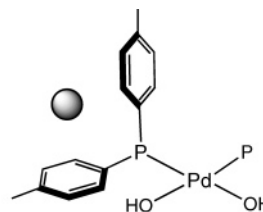


Figure 8. HOESY spectra for **2a'** (CF_3SO_3) and **2c'** (BF_4). The spectra show selective contacts to both the equatorial and axial P-phenyl ring protons.

the DFT calculations, we suggest that the anions approach the positive phosphorus and metal centers in such a way as to see both rings, perhaps as suggested by fragment **9**.



9 fragment of the dinuclear complex

Diffusion data for the CF_3SO_3 anions of the bridging anilide salts, **3a–3c**, in both dichloromethane and THF are given in Table 4. In dichloromethane solution, the D and r_{H} values are in good agreement with what one would expect on the basis of the X-ray data for **3b**. The slight increase in size, relative to, for example, **2a**, is likely related to the added anilide fragment. The r_{H} values for the CF_3SO_3 , ca. 5.6–5.7 Å, are similar to those found for **2a**. Changing the solvent to THF again results in an increase in the size of the cation due to the change in the ion pairing. The ^1H , ^{19}F HOESY spectra for **3c** in both solvents reveal five to six strong contacts in the aromatic region; however due to the low symmetry of this complex, there is a great deal of overlap and these aromatic protons cannot be readily assigned.

Table 4 also shows diffusion data for the dinuclear salt $[\text{Pd}(\mu\text{-O}_2\text{PF}_2)(\text{BINAP})_2](\text{PF}_6)_2$, **4**, and the D and r_{H} values are consistent with the related dinuclear species reported in Tables 3 and 4.

Conclusions

The various cations do not all behave identically toward the anions in this study. The PF_6 anion is readily hydrolyzed by the cation of **1**, whereas the anions CF_3SO_3 and BF_4 hydrogen-bond to the water ligands and are relatively stable. There is not much H-bonding of the anions in the dinuclear $\mu\text{-OH}$ salts **2**,

and the anion selects an approach path toward the P atoms that brings it between the two P-aryl moieties. The bridged dinuclear salts, **3**, form readily from **2** by addition of an aniline and reveal diffusion characteristics that are similar to **2**. Where measurable, the solvent THF promotes more ion pairing than does dichloromethane.

Experimental Section

General Comments. All air-sensitive manipulations were carried out under a nitrogen atmosphere. All solvents were dried over appropriate drying agents, distilled under nitrogen. Deuterated solvents were dried by distillation over molecular sieves and stored under nitrogen. The ligands *rac*-BINAP (Strem), *p*-tolyl-BINAP (Merck), and the silver salts (Aldrich) were purchased from commercial sources and used as received. The dichloro-metal complexes PdCl₂L₂ (L₂ = *rac*-BINAP or *p*-tolyl-BINAP) as well as the dications were synthesized following literature procedures.^{23b} The palladium complexes **1b** and **2b** were also prepared by a similar method. ¹H, ³¹P, ¹⁹F, and ¹⁵N NMR spectra were recorded with Bruker DPX-300, 400, and 500 MHz spectrometers at room temperature unless otherwise noted. Elemental analysis and mass spectra were performed at ETH Zürich.

Diffusion Measurements. All the measurements were performed on a Bruker Avance spectrometer, 400 MHz, equipped with a microprocessor-controlled gradient unit and a multinuclear inverse probe with an actively shielded Z-gradient coil. The gradient shape is rectangular, and its length was 1.75 ms. The gradient strength was increased by steps of 4% during the course of the experiment. The time between midpoints of the gradients was 167.75 ms for all experiments. The experiments were carried out at a set temperature of 300 K within the NMR probe.

As indicated in Tables 2–4, diffusion values were measured on 2 mM THF-*d*₈ and CD₂Cl₂ solutions. Cation diffusion rates were measured using the ¹H signal from the aromatic protons, and hydroxo-protons for **2a** or CH₃ protons for **3b** and **3c**. Anion diffusion was obtained from the ¹⁹F resonances. The error in the *D* values is thought to be ±0.06. The solvent viscosities used for the calculation of *r*_H were 0.410 and 0.456 for CD₂Cl₂ and THF-*d*₈, respectively.

NOE Measurements. The ¹H NOESY experiments^{53a} were acquired using a standard three-pulse sequence. ¹⁹F, ¹H HOESY

NMR experiments^{53b} were acquired using the standard four-pulse sequence and carried out using a doubly tuned TXI probe. A mixing time of 800 ms was used, and 16 scans were taken for each of the 512 *t*₁ increments recorded. The relevant ¹H *T*₁ values are an average of 1.7 s for the aromatic signals and 430 ms for the coordinated H₂O for **1a**. Analogous values are 1.6 s and 305 ms for **1c**. The ¹H *T*₁ value is 1.6 s for the bridging OH for **2a'**. The analogous value is 1.3 s for **2c'**. All ¹H *T*₁ values were measured in CD₂Cl₂ and calculated using the Bruker Xwin-NMR software.

Solid-State Structure of 3b. Orange-red crystals of [Pd₂(μ-OH)-(μ-{NH(*p*-Tol))}(BINAP)₂](CF₃SO₃)₂·2THF were obtained from a THF solution, which was layered with *n*-hexane. To avoid quality degradation, the single crystals were mounted in perfluoropolyalkyl ether oil on top of a glass fiber and then brought into the cold nitrogen stream of a low-temperature device so that the oil solidified. C₁₀₅H₈₉F₆NO₉P₄Pd₂S₂, triclinic, space group *P*1; *a* = 1263.4(1) pm, *b* = 1310.8(1) pm, *c* = 3038.9(2) pm; α = 80.198(1)°, β = 83.597(1)°, γ = 75.799(1)°; *V* = 4794.7(6) × 10⁶ pm³; *Z* = 2; ρ_{calcd} = 1.402 g cm⁻³; crystal dimensions 0.53 × 0.33 × 0.18 mm; diffractometer Bruker Apex with CCD detector; Mo Kα radiation, 200 K, 2θ_{max} = 56.72°; 49 678 reflections, 23 674 independent (*R*_{int} = 0.0426), empirical absorption correction SADABS (ver. 2.03), Patterson, refinement against full matrix (versus *F*²) with SHELXTL (ver. 6.12) and SHELXL-97, 1236 parameters, *R*₁ = 0.0763 and *wR*₂ (all data) = 0.2294, max./min. residual electron density 2.623/−0.835 e × 10⁻⁶ pm⁻³. All non-hydrogen atoms were refined anisotropically; however, the two crystal solvent molecules, the two SO₃CF₃⁻ (OTf⁻) counteranions, and one BINAP–P phenyl ring (C20 to C25) could properly be refined only by using the ISOR restraint.⁵⁴ The contribution of the hydrogen atoms, in their calculated positions, was included in the refinement using a riding model. One of the OTf⁻ counteranions was displaced over two positions, which were refined against each other (*F*VAR = 0.54). Upon convergence, the final Fourier difference map of the X-ray structures of **3b** showed some residual electron density close to the heavy atom palladium (~0.85 Å) or one distorted OTf⁻ position even when an absorption correction was applied. We cannot exclude further disorder for one CF₃SO₃ anion; however, this could not be refined appropriately. Crystallographic data (excluding structure factors) for the structures reported in this paper have been deposited with the Cambridge Crystallographic Data Centre as supplementary publication no. CCDC-604893 and are compiled as cif files in the Supporting Information. Copies of the data can be obtained free of charge on application to CCDC, 12 Union Road, Cambridge CB2 1EZ, UK (fax: (+44) 1223-336-033; e-mail: deposit@ccdc.cam.ac.uk).

Computational Details. The calculations were performed using the Gaussian 98 software package⁴⁴ and the B3LYP hybrid functional. This functional includes a mixture of Hartree–Fock⁴⁵ exchange with DFT⁴¹ exchange–correlation, given by Becke's three-parameter functional⁴⁶ with the Lee, Yang, and Parr correlation functional, which includes both local and nonlocal terms.^{47,48} The LanL2DZ basis set⁴⁹ augmented with an f-polarization function⁵⁰ was used for Pd, and the same basis set augmented with a d-polarization function⁵¹ was used for P; the remaining elements were described by a standard 4-31G(d)⁵² basis set. The optimizations

(44) Frisch, M. J.; Trucks, G. W.; Schlegel, H. B.; Scuseria, G. E.; Robb, M. A.; Cheeseman, J. R.; Zakrzewski, V. G.; Montgomery, J. A., Jr.; Stratmann, R. E.; Burant, J. C.; Dapprich, S.; Millam, J. M.; Daniels, A. D.; Kudin, K. N.; Strain, M. C.; Farkas, O.; Tomasi, J.; Barone, V.; Cossi, M.; Cammi, R.; Mennucci, B.; Pomelli, C.; Adamo, C.; Clifford, S.; Ochterski, J.; Petersson, G. A.; Ayala, P. Y.; Cui, Q.; Morokuma, K.; Malick, D. K.; Rabuck, A. D.; Raghavachari, K.; Foresman, J. B.; Cioslowski, J.; Ortiz, J. V.; Stefanov, B. B.; Liu, G.; Liashenko, A.; Piskorz, P.; Komaromi, I.; Gomperts, R.; Martin, R. L.; Fox, D. J.; Keith, T.; Al-Laham, M. A.; Peng, C. Y.; Nanayakkara, A.; Gonzalez, C.; Challacombe, M.; Gill, P. M. W.; Johnson, B. G.; Chen, W.; Wong, M. W.; Andres, J. L.; Head-Gordon, M.; Replogle, E. S.; Pople, J. A. *Gaussian 98*, revision A.7; Gaussian, Inc.: Pittsburgh, PA, 1998.

(45) Hehre, W. J.; Radom, L.; Schleyer, P. v. R.; Pople, J. A. *Ab Initio Molecular Orbital Theory*; John Wiley & Sons: New York, 1986.

(46) Becke, A. D. *J. Chem. Phys.* **1993**, *98*, 5648.

(47) Michlich, B.; Savin, A.; Stoll, H.; Preuss, H. *Chem. Phys. Lett.* **1989**, *157*, 200.

(48) Lee, C.; Yang, W.; Parr, G. *Phys. Rev. B* **1988**, *37*, 785.

(49) (a) Dunning, T. H., Jr.; Hay, P. J. *Modern Theoretical Chemistry*; Schaefer, H. F., III, Ed.; Plenum: New York, 1976; Vol. 3, p 1. (b) Hay P. J.; Wadt, W. R. *J. Chem. Phys.* **1985**, *82*, 270. (c) Wadt W. R.; Hay, P. J. *J. Chem. Phys.* **1985**, *82*, 284. (d) Hay P. J.; Wadt, W. R. *J. Chem. Phys.* **1985**, *82*, 2299.

(50) Ehlers, A. W.; Böhme, M.; Dapprich, S.; Gobbi, A.; Höllwarth, A.; Jonas, V.; Köhler, K. F.; Stegmann, R.; Veldkamp, A.; Frenking, G. *Chem. Phys. Lett.* **1993**, *208*, 111.

(51) Höllwarth, A.; Böhme, M.; Dapprich, S.; Ehlers, A. W.; Gobbi, A.; Jonas, V.; Köhler, K. F.; Stegmann, R.; Veldkamp, A.; Frenking, G. *Chem. Phys. Lett.* **1993**, *208*, 237.

(52) (a) Ditchfield, R.; Hehre W. J.; Pople, J. A. *J. Chem. Phys.* **1971**, *54*, 724. (b) Hehre, W. J.; Ditchfield R.; Pople, J. A. *J. Chem. Phys.* **1972**, *56*, 2257. (c) Hariharan, P. C.; Pople, J. A. *Mol. Phys.* **1974**, *27*, 209. (d) Gordon, M. S. *Chem. Phys. Lett.* **1980**, *76*, 163.

(53) (a) Jeener, J.; Maier, B. H.; Bachmann, P.; Ernst, R. R. *J. Chem. Phys.* **1979**, *71*, 4546. (b) Lix, B.; Sönnichsen, F. D.; Sykes, B. D. *J. Magn. Reson., Ser. A* **1996**, *121*, 83.

(54) The named atoms are *restrained* with effective standard deviations so that their *U*_{*ij*} components approximate to isotropic behavior; however the corresponding isotropic *U* is free to vary. ISOR is often applied, perhaps together with SIMU, to allow anisotropic refinement of large organic molecules when the data are not adequate for unrestrained refinement of all the *U*_{*ij*}.

were performed without symmetry constraints. A natural population analysis (NPA)⁴³ was used to evaluate the charge distribution on the optimized species.

[Pd(H₂O)₂(BINAP)(PF₆)₂ (1b). To a solution of PdCl₂ (*rac*-BINAP) (100 mg, 0.125 mmol) in dry acetone (50 mL) were added water (0.045 mL, 20 equiv) and AgPF₆ (70 mg, 2.5 mmol, 2.2 equiv) at 25 °C. The reaction mixture was then stirred at 25 °C for 3 h. The precipitate of AgCl was filtered over Celite, and the solvent was concentrated under vacuum. The crude product was obtained as a yellow solid. Yield: 192 mg, 0.182 mol, 97%. ¹H NMR (THF-*d*₈, 400 MHz, 25 °C): δ 2.65 (br s, 4H), 6.6–8.3 (m, 32H). ³¹P-{¹H} NMR (THF-*d*₈, 161 MHz, 25 °C): δ 34.3 ppm (s), -144 (sept, ¹J_{FP} = 712 Hz). ¹⁹F NMR (THF-*d*₈, 282 MHz, 25 °C): δ -74 (d, ¹J_{FP} = 712 Hz). ESI-MS (*m/z*) Pd (BINAP): 727; BINAP - PPh₂: 437; Pd (BINAP)(H₂O)₂: 763.

[Pd(μ-OH)(BINAP)]₂(PF₆)₂ (2b). To a solution of **1b** (97 mg, 0.092 mmol) in dry acetone (15 mL) was added dried 4 Å molecular sieves (1–2 mm, 1 g). The reaction mixture was stirred at 25 °C for 3 h. After filtration over Celite, the acetone was concentrated under vacuum. The crude product was obtained as an orange solid. Yield: 19 mg, 0.01 mol 23%. ¹H NMR (CD₂Cl₂, 400 MHz, 25 °C): δ -2.9 (br s, 2H), 6.6–7.8 (m, 64H). ³¹P{¹H} NMR (CD₂-Cl₂, 161 MHz, 25 °C): δ 29.3 ppm (s), -144 (sept, ¹J_{FP} = 711 Hz). ¹⁹F NMR (CD₂Cl₂, 282 MHz, 25 °C): δ -73 (d, ¹J_{FP} = 711 Hz). ESI-MS (*m/z*) M⁺ - PF₆ - 2OH: 1457; M⁺ - PF₆ - PPh₂: 1273; M⁺ - PF₆ - 2OH - BINAP + PPh₂: 1021; Pd (BINAP): 727; BINAP - PPh₂: 437

[Pd₂(μ-OH)(μ-{NH(*p*-ClC₆H₄)})](BINAP)₂(CF₃SO₃)₂ (3a). To a solution of **2a** (100 mg, 0.056 mmol) in THF (10 mL) was added *p*-chloroaniline (57 mg, 0.445 mmol). The reaction mixture was stirred at 25 °C for 3 h, during which time a clear red solution was obtained. The THF was then concentrated under vacuum. The crude solid was washed with pentane and then dried in vacuo. The product, **3a**, was obtained as an orange solid. Yield: 101 mg, 0.053 mmol, 95%. The product was recrystallized from a THF–pentane solution. ESI-MS M⁺: 1750; M⁺ - OTf⁻: 1600; Pd(BINAP)-(Aniline): 856; Pd(BINAP)(OH): 744; BINAP - PPh₂: 437. ¹H NMR (298 K, THF-*d*₈): -3.74 (dd, ³J_{HP} = 2.7, ³J_{HP} = 2.7, OH), 6.48–7.96 (m, 69 H). ¹⁹F NMR (298 K, THF-*d*₈): -78 (s, CF₃). ³¹P NMR (298 K, THF-*d*₈): 25.0 (dd, ²J_{PP} = 23.2, ⁴J_{PP} = 5.8), 25.5 (d, ²J_{PP} = 24.1), 26.3 (d, ²J_{PP} = 23.1), 27.7 (dd, ²J_{PP} = 24.2, ⁴J_{PP} = 5.8). ¹⁵N NMR (213 K, CD₂Cl₂): 30.0 (NH₂C₆H₄Cl), 55.1 (μ-NHC₆H₄Cl).

[Pd₂(μ-OH)(μ-{NH(*p*-Tol)})](BINAP)₂(CF₃SO₃)₂ (3b). To a solution of **2a** (100 mg, 0.056 mmol) in THF (15 mL) was added *p*-methylaniline (51.2 mg, 0.479 mmol). The reaction mixture was stirred at 25 °C for 3 h, during which time a clear red solution was obtained in THF. The THF was then concentrated under vacuum. The crude solid was washed with ET₂O and then dried in vacuo.

The product, **3b**, was obtained as a red solid. Yield: 49 mg, 0.026 mmol, 47%. Red needles were obtained from recrystallization from a THF–ET₂O solution. ESI-MS M⁺: 1729; Pd(BINAP)-(Aniline): 834; Pd(BINAP)(OH): 744; BINAP - PPh₂: 437. ¹H NMR (298 K, THF-*d*₈): -3.86 (dd, ³J_{HP} = 2.9, ³J_{HP} = 2.9, OH), 6.41–7.96 (m, 69 H). ¹⁹F NMR (298 K, THF-*d*₈): -78 (s, CF₃). ³¹P NMR (298 K, THF-*d*₈): 24.6 (dd, ²J_{PP} = 23.5, ⁴J_{PP} = 5.8), 25.1 (d, ²J_{PP} = 26.3), 26.5 (d, ²J_{PP} = 23.6), 27.7 (dd, ²J_{PP} = 26.1, ⁴J_{PP} = 5.8).

[Pd₂(μ-OH)(μ-NH-*p*-MeO-C₆H₄)(BINAP)₂](CF₃SO₃)₂ (3c). To a solution of **2a** (100 mg, 0.056 mmol) in THF (10 mL) was added *p*-methoxyaniline (60 mg, 0.488 mmol). The reaction mixture was stirred at 25 °C for 3 h, during which time a dark red suspension was obtained in THF. The THF was then concentrated under vacuum. The crude solid was washed with ET₂O and then dried in vacuo. The product, **3c**, was obtained as a dark red solid. Yield: 103 mg, 0.054 mmol, 97%. ESI-MS M⁺: 1746; Pd(BINAP)-(Aniline): 850; Pd(BINAP)(OH): 744; BINAP - PPh₂: 437. ¹H NMR (298 K, THF-*d*₈): -3.97 (dd, ³J_{HP} = 2.7, ³J_{HP} = 2.7, OH), 6.43–8.04 (m, 69 H). ¹⁹F NMR (298 K, THF-*d*₈): -78 (s, CF₃). ³¹P NMR (298 K, THF-*d*₈): 24.3 (dd, ²J_{PP} = 25.4, ⁴J_{PP} = 5.7), 25.1 (d, ²J_{PP} = 27.6), 26.6 (d, ²J_{PP} = 25.7), 27.6 (dd, ²J_{PP} = 27.2, ⁴J_{PP} = 5.7). ¹⁵N NMR (213 K, CD₂Cl₂): 28.6 (NH₂C₆H₄Cl) 52.5 (μ-NHC₆H₄Cl).

[Pd(μ-O₂PF₂)(BINAP)]₂ (PF₆)₂ (4). To 1 equiv of [Pd Cl₂ (*rac*-BINAP)] (46.5 mg, 800.01 g mol⁻¹, 58.1 × 10⁻³ mol) were added 2 equiv of AgPF₆ (30.8 6 mg, 252.86 g mol⁻¹) in wet acetone. The reaction mixture was stirred at 25 °C for 3 h. After this time, the yellow solution was evaporated under reduced pressure and dried under vacuum to afford the product, **4**, as a yellow powder. Yield: 48 mg, 0.025 mol, 84%. ¹H NMR (CD₂Cl₂, 400 MHz, 25 °C): 6.7–7.8 (m, 64H). ³¹P{¹H} NMR (CD₂Cl₂, 161 MHz, 25 °C): δ 33.3 ppm (s) -15.5 (t, ¹J_{PF} = 962 Hz), -144.1 (sept, ¹J_{PF} = 707 Hz). ¹⁹F NMR (CD₂Cl₂, 282 MHz, 25 °C): δ -73 (d, ¹J = 707 Hz), -83 (d, ¹J = 962 Hz). ESI-MS M⁺: 930, [Pd(μ-O₂PF₂)-(BINAP)]₂. Anal. {found (calcd)} C {54.09 (54.20)} H {3.34- (3.31)}.

Acknowledgment. P.S.P. thanks the Swiss National Science Foundation and the ETH Zurich for support, as well as the Johnson Matthey Company for the loan of palladium salts. We also thank Prof. Frank Breher for determining the structure of **3b**, Mr. Julian Schwartz for the synthesis of **3b**, and Dr. K. K. (Mimi) Hii for helpful discussions.

Supporting Information Available: Figures (S1 and S2) with the DFT structures of the mononuclear species and tables of atomic coordinates for all the optimized species. This material is available free of charge via the Internet at <http://pubs.acs.org>.

OM0603518